

# NASA Technical Memorandum 85700

NASA-TM-85700 19840003152

## SURFACE ANALYSIS OF GRAPHITE REINFORCED POLYIMIDE COMPOSITES

FOR REFERENCE  
NOT TO BE REPRODUCED FROM THIS ROOM

D. L. Messick, D. J. Progar and J. P. Wightman

OCTOBER 1983

LIBRARY COPY

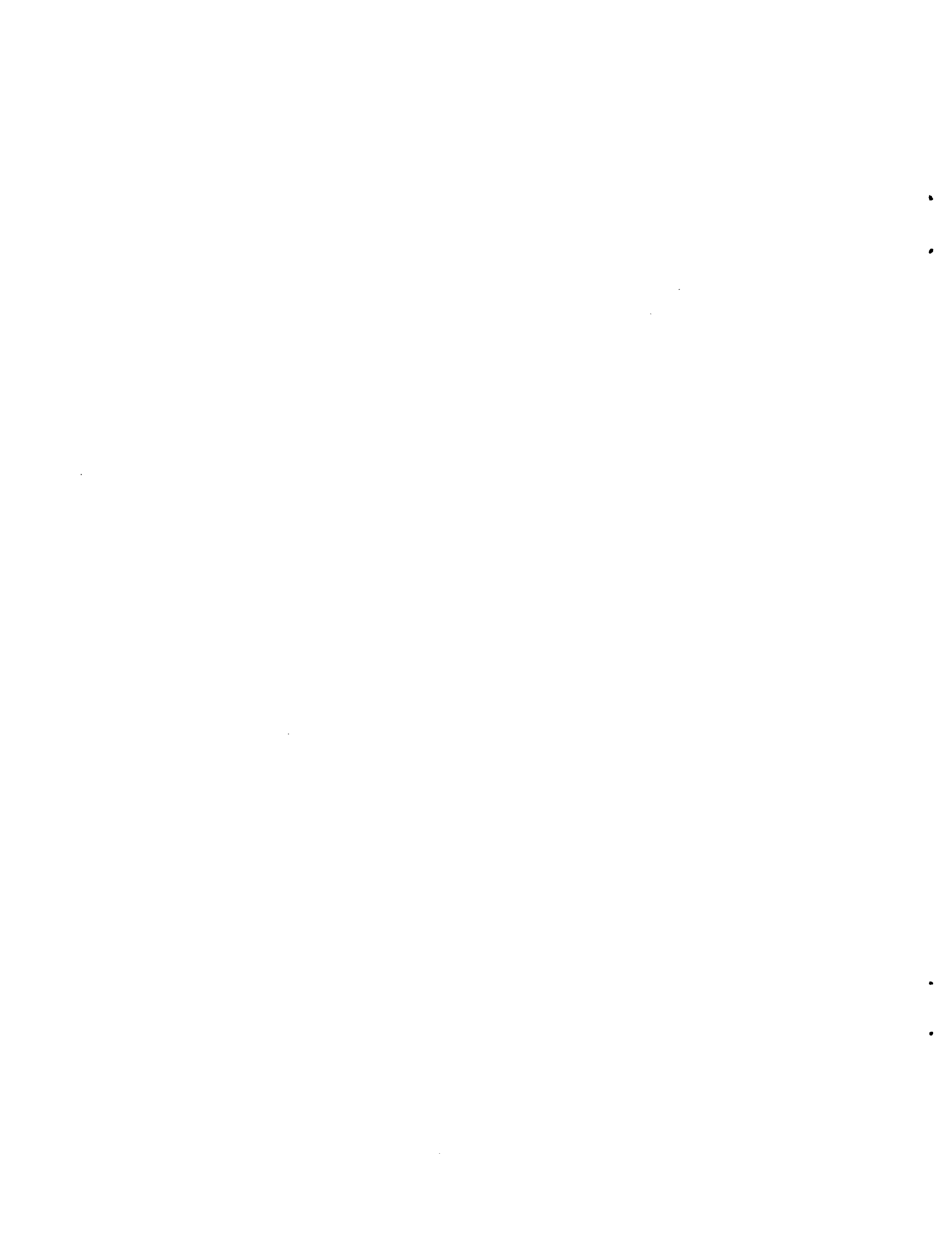
OCT 1983

LANGLEY RESEARCH CENTER  
LIBRARY, NASA  
HAMPTON, VIRGINIA



National Aeronautics and  
Space Administration

Langley Research Center  
Hampton, Virginia 23665



## 1. INTRODUCTION

Langley Research Center (LaRC) has been actively engaged in advancing composites and composite structures technology for the past decade. Several large LaRC composite application programs such as CASTS, SCR, and ACEE, have had a significant impact in extending the use of composites in aircraft and spacecraft structures. The use of composite materials has many advantages over metallic structures; for example, composite structures almost always result in significant weight savings, cost savings, and a reduction in the total number of components when compared to metallic designs. Efficient joining methods are of primary importance for the increased use of composite materials on aircraft structures. The joining techniques for composites are limited to mechanical fasteners and adhesive bonding, the latter being the preferred technique. Studies utilizing epoxy matrix composites and epoxy adhesives have been widely reported in the literature; however, there is a lack of information on studies using high temperature composites and adhesives. The development of efficient joining procedures for high temperature composites, i.e., graphite/polyimide, is very important for the fabrication of advanced aerospace structures. The long term objective of this study

is to establish the effect of composite surface treatments on the strength and durability of high temperature adhesive bonded graphite polyimide structures.

Crane et al. (1) studied the effect of peel ply, chemical, and mechanical surface treatments on the wettability and bondability of a cured epoxy/graphite composite with Narmo 329-1C epoxy adhesive. Their results indicate no obvious correlation between surface energetics and bond strength. Of the surface treatments studied, the sanded surface gave improved bond strength compared to the untreated sample.

Pater and Scola (2) using Fourier transform infrared spectroscopy, studied surface contamination from the transfer of various release agents to the composite surface during fabrication of a series of Kevlar, glass, and graphite/epoxy composites. The type of mold, mold surface treatments, release agent used, and reinforcing fibers were the factors found to influence the amount of release agent transfer. Adhesive bonding to the composite was not addressed in the report.

The effect of the degree of abrasion obtained by alumina grit blasting of epoxy composite surfaces on the strengths of epoxy

bonded joints was studied by Stone (3). Incomplete abrasion of composite surfaces resulted in reduced joint strength for some adhesives, as well as a high proportion of composite/primer interface failure, probably due to polytetrafluoroethylene residues from the release cloths during fabrication.

Parker and Waghorne (4) also studied carbon fiber-reinforced composite laminates that were molded against release cloths, metal plates coated with release agents, and sheets of silicone rubber. X-ray photoelectron spectroscopy (XPS or ESCA) was used to investigate the chemical composition of the surfaces and indicated contamination by release agents during fabrication which resulted in reduced strengths for epoxy adhesive-bonded joints. Abrasion by various methods reduced, but did not eliminate, the contamination.

There is a continuing need to establish the role of the interfacial region in determining the bond strength and durability of composite bonds. Preliminary studies (5,6) on the characterization of a variety of graphite fibers including Celion 6000 using both scanning electron microscopy (SEM) and x-ray photoelectron spectroscopy (XPS) have been

reported. Donnet has emphasized recently (7) the importance of the surface characterization of fibers in attempting to understand the properties of composites. However, the emphasis in the present work is on composite bonding, that is, the adhesive bonding between composites in contrast to fiber-matrix interaction. The primary objective of the research is the characterization of composite surfaces before adhesive bonding. This paper details work done on the analysis of composite samples pretreated in a number of ways prior to bonding.

## 2. EXPERIMENTAL

### 2.1 Samples.

The composites were made by Rockwell International from Celion 6000 graphite fibers with a NR 150B2 polyimide finish in a polyimide (LARC-160) matrix. Figures 1(a) and 1(b) illustrate the fabrication process used by Rockwell International to make the Celion 6000/LARC-160 composites used for the present study. Prepreg was supplied to Rockwell International by Fiberite. Figure 1(a) shows the vacuum bag layup used for the prepreg compaction step (or debulking step). Note the teflon coated glass fabric (3TLL) in contact with the prepreg during processing. The staging conditions are given in Figure 1(b). A similar vacuum bag arrangement was used for the curing step (Figure 2). The materials

used for the curing step must be stable at the higher temperature of 329°C (625°F) than for the previous step. Teflon coated glass fabric was again in contact with the composite as was the case for the compaction step. The cure temperature profile is given in Figure 3. Full vacuum and 738 kPa (200 psi) pressure are held throughout the cure cycle. Properties of the composites are given in Table I.

The composites were pretreated in the twelve different ways listed in the second column of Table II. Details of each pretreatment are given below. Sample No. 2 was lightly (2-3 quick passes) blasted using 120 grit alumina and air pressure of 90 psi with the nozzle held approximately 8-10 inches from the sample. Sample No. 3 was blasted using 100 grit alumina and air pressure of 15 psi. Sample No. 4 was lightly (one pass) blasted with 88-140 $\mu$  diameter glass beads in a dry honer with the nozzle held about 12 inches from the surface. Sample No. 5 was handsanded manually using 600 SiC sandpaper. Sample No. 6 was handsanded manually in a criss-cross pattern with 180 SiC sandpaper. Ethanolic KOH solution at room temperature was spread on Sample No. 7 and soaked for 2-3 minutes. Additional ethanolic KOH solution was spread and soaked for

2-3 minutes. Sample was then rinsed with distilled water and blow dried. Hydrazine hydrate at room temperature was spread on Sample No. 8, soaked for 15 minutes, rinsed with distilled water and blow dried. A 50/50 (by volume) solution of concd. H<sub>2</sub>SO<sub>4</sub> and 30% H<sub>2</sub>O<sub>2</sub> at room temperature was spread on Sample No. 9, soaked for 30 minutes, rinsed with distilled water and blow dried. Samples Nos. 10-12 were irradiated at different fluxes using a Flashblast\*<sup>TM</sup> model FB-200 to obtain 14, 24 and 40 J/cm<sup>2</sup>. Sample No. 12 following irradiation was washed with methanol to remove residue and the washed sample was coded Sample No. 12W.

A 0.5 cm (0.2 in) diameter sample was punched from each composite and photographed at 20X with a Bausch and Lomb optical microscope prior to any analysis. The as-received sample designated Sample No. 1A delaminated on punching and hence a virgin internal surface was produced and designated Sample No. 1B.

## 2.2 Scanning Electron Microscopy/ Energy Dispersive Analysis of X-rays (SEM/EDAX).

Photomicrographs were obtained using a Polaroid camera back attached to the oscilloscope on the Advanced Metals Research Corporation Model 1000 scanning electron

\*Flashblast is the official trademark of Maxwell Laboratories Inc.

microscope (AMR 1000 SEM). Operating at 20 kV, high magnification views (500X-5000X) gave information on the details of surface features, while survey scans at 20X-200X provided a check on the distribution of representative features that describe the surface. For convenience in studying the results, approximate horizontal dimensions of each photomicrograph appear at the right in the figures 4-9.

Specimens were cut to approximately 1 x 1 cm (0.4 x 0.4 in) on a diamond wheel saw and fastened to SEM mounting stubs with metal clamps. To enhance conductivity of the composite samples, a thin (~20 nm) film of Au was vacuum-evaporated (Technics, Model Hummer I) onto the samples which had been ultrasonically cleaned in methanol. Photomicrographs were taken with the sample inclined 30° from the incident electron beam. Rapid, semiquantitative elemental analyses were obtained with an EDAX International Model 707A energy-dispersive x-ray fluorescence analyzer attached to the microscope. Detection was limited to elements of atomic number 11 (Na) and above. A Polaroid photographic record of each spectrum was made using a camera specially adapted for the EDAX oscilloscope

output.

### 2.3 X-ray Photoelectron Spectroscopy (XPS).

XPS studies of the composites were obtained with a Physical Electronics SAM 550 spectrometer using a Mg x-ray anode. Punched samples were mounted to the XPS stage with double-sided tape. A wide scan of binding energies (0 to 1000 eV) was performed on Sample Nos. 1A and 1B initially. Subsequent narrow scans were completed for the elements C, N, O, S, F, Al, Si, and K on all samples. The atomic fraction of each of these elements present in the top 5 nm of the surface was calculated.

### 2.4 Contact Angles.

Five different liquids of varying surface tensions were used for contact angle determinations. The liquids and respective surface tensions (in mJ/m<sup>2</sup>) are noted below: water (72.8), formamide (58.3), methylene iodide (50.8), bromonaphthalene (44.6), n-hexadecane (27.6). A droplet of each liquid approximately 5 mm in diameter was placed on each composite sheet. Contact angles were measured with a Gaertner Scientific goniometer within 30 seconds after the introduction of the droplet. A second replication was completed for each liquid on each composite. Means were calculated using the University IBM 1360 com-

puter system which was also used to construct plots of measured contact angle ( $\theta$ ) as a function of surface tension ( $\gamma$ ). Critical surface tensions for each composite were obtained by extrapolation of  $\cos \theta$  vs  $\gamma$  plots using the Zisman approach (8).

### 3. RESULTS AND DISCUSSION

#### 3.1 Scanning Electron Microscopy/ Energy Dispersive Analysis of X-rays (SEM/EDAX)

SEM photomicrographs (100x, 500x, and 5000x) were used to assess changes in surface topography of composite samples after different pretreatments. The surface of Sample No. 1A (as-received) shown in Figure 4(a) contains polymer-rich "peaks" and polymer-poor "valleys" which had conformed to the pattern of the release cloth used during fabrication. Figure 4(b) shows a smooth polymer transition region between a peak and valley. The apex of a peak with cracks (fissures) in the polymer is shown in Figure 4(c). The graphite fibers close to the surface are covered with a thin coating of matrix polymer as evidenced in Figure 4(d). This composite surface, Sample No. 1A, was the as-received surface to which the different pretreatments were given.

An edge view of Sample No. 1A indicates a highly-compacted void-free composite (Figure 5 (a)).

The spherical shapes on the right of Figure 5 (a) are the acrylic molding material used to mount the sample during polishing. The varying thicknesses of the surface polymer is evident in the figure and varies according to the location of the cut through the composite. Figure 5(b) is a higher magnification showing the range of thickness for the surface polymer in greater detail.

The surface of Sample No. 2 was obtained by grit blasting with 120 alumina grit and a very rough surface with fiber damage and polymer breakup was obtained (Figure 6 (a)). The brittle nature of the polymer matrix and the polymer-rich and polymer-poor areas is still evident. The transition region between the polymer-rich and polymer-poor areas is shown in Figure 6(b). Figures 6(c) and 6(d) are of the peak and valley areas, respectively. The removal of the thin polymer coating on the fibers, thus exposing apparent "clean" graphite fibers, can be seen in Figure 6(d). The surfaces of Sample Nos. 3 and 4 are very similar to Sample No. 2 and therefore the photomicrographs are not reproduced here.

The surface produced by manually abrading with 600 SiC sandpaper, Sample No. 5, is shown in Figure 7. Figure 7(a) shows that the

treatment removed the polymer peaks down to the graphite fibers with little damage to the fibers when compared to the 120 grit blasted surface. The valleys remain almost intact in most areas of the treated surface. Figure 7(b) is the transition region between polymer-rich and polymer-poor areas. As noted in Figure 7(c), the resin is separated from the fibers in some cases due to the abrasive action. The surface of Sample No. 6 was obtained in a similar fashion to Sample No. 5 except that 180 SiC sandpaper was used, producing the surface shown in Figure 8 (a). A criss-cross abrasive pattern was used to generate the rough surface which produced significant damage to the fibers, (polymer-rich area, Figure 8(c) and polymer-poor area, Figure 8(d)). The transition region between polymer-rich and polymer-poor areas appears in Figure 8(b).

The Flashblast™ process, performed by Maxwell Laboratories Inc. for LaRC, produces a surface (Sample No. 12W) significantly different than the other surface treatments. The Flashblast process consists of subjecting the surface to intense light energies to vaporize or chemically alter

the surface. The residue produced during the process was removed by washing with methanol while stroking with a natural bristle paint brush. Some polymer has been removed from the surface leaving a pitted surface on the polymer peaks (Figures 9 (a), (b), and (c)), and a thin-walled cellular structure between the graphite fibers (Figure 9 (d)). The cellular structure appears to be composed of both open and closed cells. For some surface areas of the fibers, the polymer appears to be completely removed.

Photomicrographs of the surfaces of Samples Nos. 7, 8 and 9 which were given different chemical pretreatments all appear similar to those for Sample No. 1A and therefore are not reproduced in this paper. Overall, mechanically and light irradiated samples showed varying degrees of the polymer peak removal; as-received and chemically pretreated samples showed polymer-rich "peaks" and polymer-poor "valleys". Results of EDAX analysis indicate the presence of a small amount of silicon for all the surfaces of Sample Nos. 1A, 2-9, and 12W. The presence of silicon was also noted during XPS analysis (< 1.3 atomic percent). A trace amount of



calcium was also noted for surfaces of Sample Nos. 7 and 8. The source of silicon and calcium is uncertain.

### 3.2 X-ray Photoelectron Spectroscopy (XPS).

An extensive XPS study was done on the composite samples before and following different pretreatments. Wide scan XPS spectra were obtained on Samples Nos. 1A, 1B, 7, 8, and 9. The major photopeaks were assigned to fluorine, oxygen, nitrogen and carbon. The presence of large amounts of fluorine on the surface of some of the samples even after pretreatment is a striking result and emphasizes the importance of surface analysis in determining trace concentrations of elements on bonding surfaces which may be detrimental to bond properties. In addition, trace amounts of calcium and sodium were noted on Sample No. 7, and Sample Nos. 1A and 7, respectively.

Narrow scan XPS spectra were obtained on all samples and in addition to scanning for fluorine, oxygen, nitrogen, and carbon, scans were also made for potassium, sulfur, aluminum, and silicon. These latter elements were suspected surface impurities based on the known pretreatments. Potassium was not detected on any sample; sulfur appeared as a trace

impurity but it may be associated with the sample holder.

The quantitative results of the XPS analysis are given in Tables II and III. The binding energies (B.E.) in eV and the atomic fractions (A.F.) for the F 1s, O 1s, N 1s and C 1s photopeaks are listed in Table II. Half of the samples contained high concentrations of surface fluorine even following pretreatment and in every case, a high binding energy photopeak around 292 eV was observed in the C 1s spectrum. This is a characteristic of carbon-fluorine bonding (9). Of particular interest is the fact that the as-received composite (Sample No. 1A) has a large fluorine signal. However, the fluorine photopeak is some 100 times smaller for a freshly exposed surface (Sample No. 1B) produced on delamination of the same sample.

The atomic fraction ratios are listed in Table III. There are large differences in the F/C ratio for the various samples. The mechanically pretreated composites generally have lower F/C ratios than the chemically pretreated composites. The longer Flashblast treated samples show a much reduced fluorine signal. Further, the values of the O/C ratio are fairly constant except for the Flashblast pretreated Sample Nos. 11, 12 and 12W. A parallel trend is noted in

the N/C ratio. It appears as though the Flashblast pretreatment carbonizes the surface region resulting in the removal of oxygen and nitrogen contained in gaseous species possibly, for example, CO and HCN.

In summary, the surface fluorine is associated with the external composite surfaces only, which suggests the inclusion of fluorine during composite fabrication. The order of removal of the surface fluorine species by the treatment is, Flashblast > mechanical > chemical, with Flashblast being the most effective.

Fracture studies at NASA-LaRC have been made on similar bonded composites pretreated in the same ways as above. The effect of surface contamination on bond strength is being evaluated currently.

### 3.3 Critical Surface Tension.

The critical surface tension delineates the wettability of a solid surface. The critical surface tension of each composite sample is listed in Table III. A direct correlation is suggested between the surface fluorine concentration as measured by XPS and the value of the critical surface tension. The results of these two independent techniques are plotted in Figure 10. Indeed, the higher the surface fluorine concentration, the lower the critical surface tension.

This result is consistent with critical surface tensions reported for fluoropolymers (8).

## 4. CONCLUSIONS

This study was focused on SEM/EDAX, XPS analysis and contact angle measurements on graphite fiber composites pretreated in a number of different ways including mechanical, chemical and light irradiation. A significant fluorine signal was observed by XPS on the as-received Celion 6000/LARC-160 composite surface prior to pretreatment. Only a trace fluorine signal is noted on a delaminated surface of the same as-received sample. This result indicates that fluorine is probably introduced by contact with the Teflon coated glass fabric during the fabrication step. Chemical pretreatment was the least effective method of removing surface fluorine while the Flashblast process reduced the fluorine signal to trace levels. Critical surface tensions of the pretreated composites were determined from measured contact angles. Low critical surface tensions were characteristic of composite surfaces having high surface fluorine concentration as determined by XPS.

SEM/EDAX results of the composites clarified the topography changes resulting from the various mechanical, chemical, and light irradiated pretreatments. XPS results and contact angle measurements

produced information on the surface contamination as a result of fabrication techniques which may provide answers to the strength and durability of adhesively bonded composites. These techniques have been shown to be capable of providing valuable information with respect to surface analysis of composites prior to adhesive bonding.

#### 5. ACKNOWLEDGEMENTS

Work supported in part under NASA Grant NAG-1-248 and by the Office of Naval Research. We thank Frank Cromer of the Poly-Scientific Company for the XPS analysis.

#### 6. REFERENCES

1. L.W. Crane, C.L. Hammermesh and L. Maus, SAMPE J., 12, No. 2, 6 Mar/Apr 1976).
2. R.H. Pater and D.A. Scola, 11th National SAMPE Technical Conference, 11, 151 (1979).
3. M.H. Stone, Internatl. J. of Adhesion and Adhesives, 1, 271 (1981).
4. B.M. Parker and R.M. Waghorne, Composites, 13, 280 (1982).
5. W. Chen and J.P. Wightman, "A Fundamental Approach to Adhesion: Synthesis, Surface Analysis, Thermodynamics and Mechanics", NASA Report CR-158438, January 1979.
6. W. Chen and J.P. Wightman, Proc. 14th Biennial Conference on Carbon, P. A. Thrower, Ed., p. 107, State College, Pa. (1979).
7. J.B. Donnet, Abstracts, 4th Intl. Conference on Surface and Colloid Science, Jerusalem, July, 1981.
8. W.A. Zisman in "Contact Angle, Wettability and Adhesion", Adv. Chem. Series #43, R.F. Gould, Ed., pp. 1-51, Am. Chem. Soc., Washington (1964).
9. K.Siegbahn et al., "ESCA-Atomic, Molecular and Solid State Structure Studies by Means of Electron Spectroscopy", Almquist and Wiksells, Upsalla (1967).

TABLE I  
 PROPERTIES OF CELION 6000/LARC-160 COMPOSITE

Panel No.	T <sub>g</sub> (°C)	Average Thickness(mm)	Specific Gravity	V <sub>F</sub> %	Void %
1	344 (651°F)	2.2 (0.086 in)	1.57	59	0.1
2	332 (629°F)	2.0 (0.079 in)	1.58	61	<1.0

a (0,0,0,+30,-30,+30,-30)<sub>s</sub> ply orientation.

TABLE II  
 XPS ANALYSIS OF COMPOSITES

Sample No.	Sample Pretreatment	Photopeak				B.E.(eV)
		F 1s	O 1s	N 1s	C 1s	
1A	As-received	689.0	531.8	399.8	(284.6)	B.E.(eV)
		0.19	0.11	0.030	0.66	A.F.
1B	Delaminated	688.8	532.4	400.2	(284.6)	
		0.002	0.11	0.020	0.86	
2	120 Al <sub>2</sub> O <sub>3</sub> Grit Blast	689.0	531.4	399.8	(284.6)	
		0.13	0.11	0.020	0.73	
3	Boeing Grit Blast	689.0	532.0	400.0	(284.6)	
		0.060	0.15	0.023	0.75	
4	Glass Bead Blast	689.2	531.8	400.0	(284.6)	
		0.12	0.12	0.024	0.73	
5	600 SiC Handsand	689.4	532.2	400.2	(284.6)	
		0.025	0.13	0.020	0.80	
6	180 SiC Handsand	689.0	531.8	400.0	(284.6)	
		0.027	0.12	0.032	0.81	
7	Ethanollic KOH	689.2	531.8	399.8	(284.6)	
		0.26	0.10	0.012	0.63	
8	NH <sub>2</sub> NH <sub>2</sub> ·H <sub>2</sub> O	689.2	531.8	399.6	(284.6)	
		0.20	0.10	0.041	0.64	
9	Concd. H <sub>2</sub> SO <sub>4</sub> + 30% H <sub>2</sub> O <sub>2</sub>	689.2	532.0	400.0	(284.6)	
		0.19	0.12	0.020	0.66	
10	Flashblast #1	689.4	532.0	400.2	(284.6)	
		0.14	0.080	0.026	0.74	
11	Flashblast #2	-	532.6	-	(284.6)	
		NSP	0.053	NSP	0.93	
12	Flashblast #3	689.2	532.4	400.0	(284.6)	
		0.006	0.078	0.010	0.89	
12W	Flashblast #3 (after MeOH wash)	-	532.4	400.0	(284.6)	
		NSP	0.071	0.021	0.89	

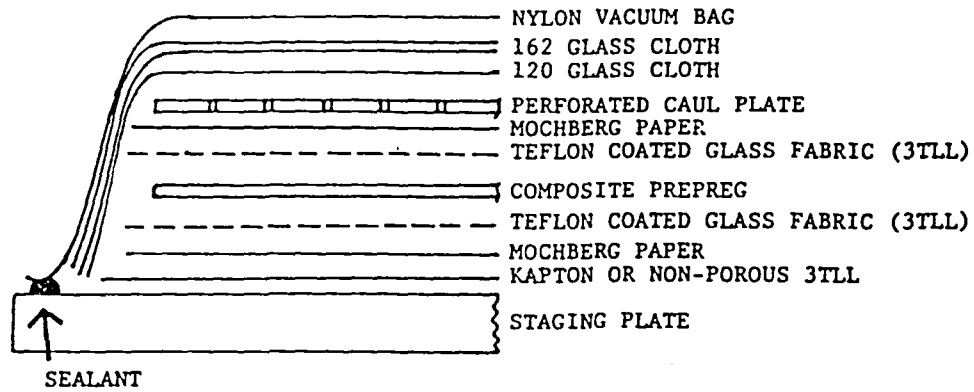
NSP - no significant peak

TABLE III

## XPS ATOMIC RATIOS AND CRITICAL SURFACE TENSIONS OF COMPOSITES

Sample No.	Atomic Fraction Ratio			Critical Surface Tension (mJ/m <sup>2</sup> )
	F/C	O/C	N/C	
1A	0.29	0.17	0.045	23.
1B	0.0023	0.13	0.023	--
2	0.18	0.15	0.027	31
3	0.08	0.20	0.031	37
4	0.16	0.16	0.032	33.
5	0.031	0.16	0.025	35.
6	0.033	0.15	0.040	40.
7	0.41	0.16	0.019	23.
8	0.31	0.16	0.064	28.
9	0.29	0.18	0.030	31.
10	0.19	0.11	0.035	37.
11	<0.001	0.057	<0.001	40.
12	0.0067	0.088	0.011	40.5
12W	<0.001	0.080	0.023	--

(a) VACUUM BAG LAYUP



(b) STAGING CONDITIONS

1. APPLY 12.7cm (5in) Hg VACUUM AND HOLD FOR FULL CYCLE.
2. HEAT TO 491K (425°F).
3. HOLD AT 491K (425°F) FOR 30 MINUTES.
4. COOL TO LESS THAN 339K (150°F) BEFORE RELEASING VACUUM.

FIGURE 1. TYPICAL (a) VACUUM BAG LAYUP AND (b) STAGING CONDITIONS FOR CELION 6000/LARC-160 COMPOSITE FABRICATION.

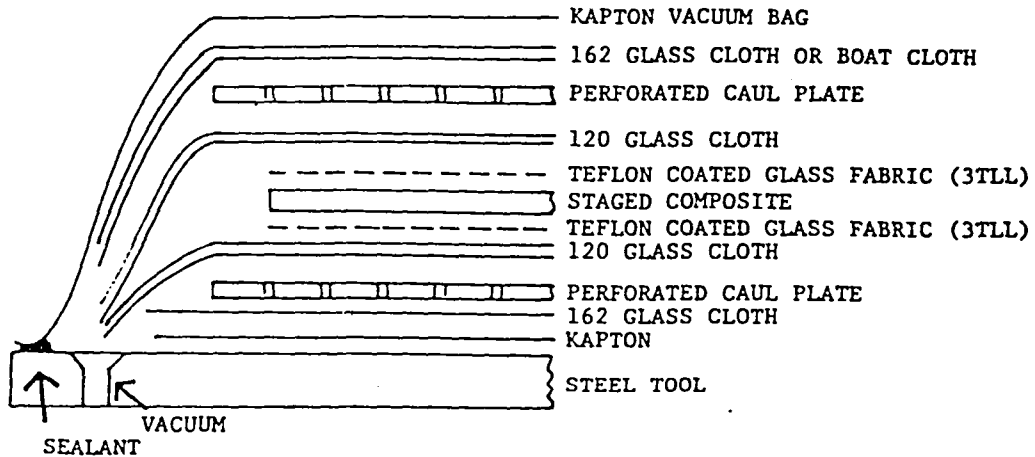


FIGURE 2. VACUUM BAG LAYUP FOR CURE PROCESS OF CELION 6000/LARC-160 COMPOSITE.

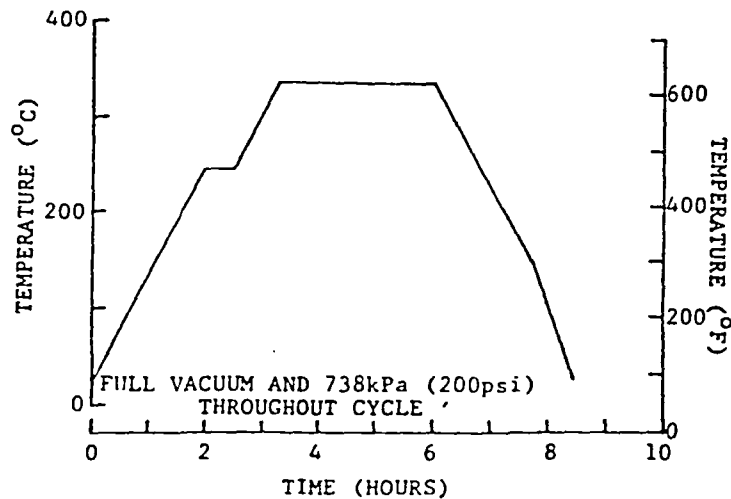


FIGURE 3. FINAL CURE CYCLE FOR CELION 6000/LARC-160 COMPOSITE.

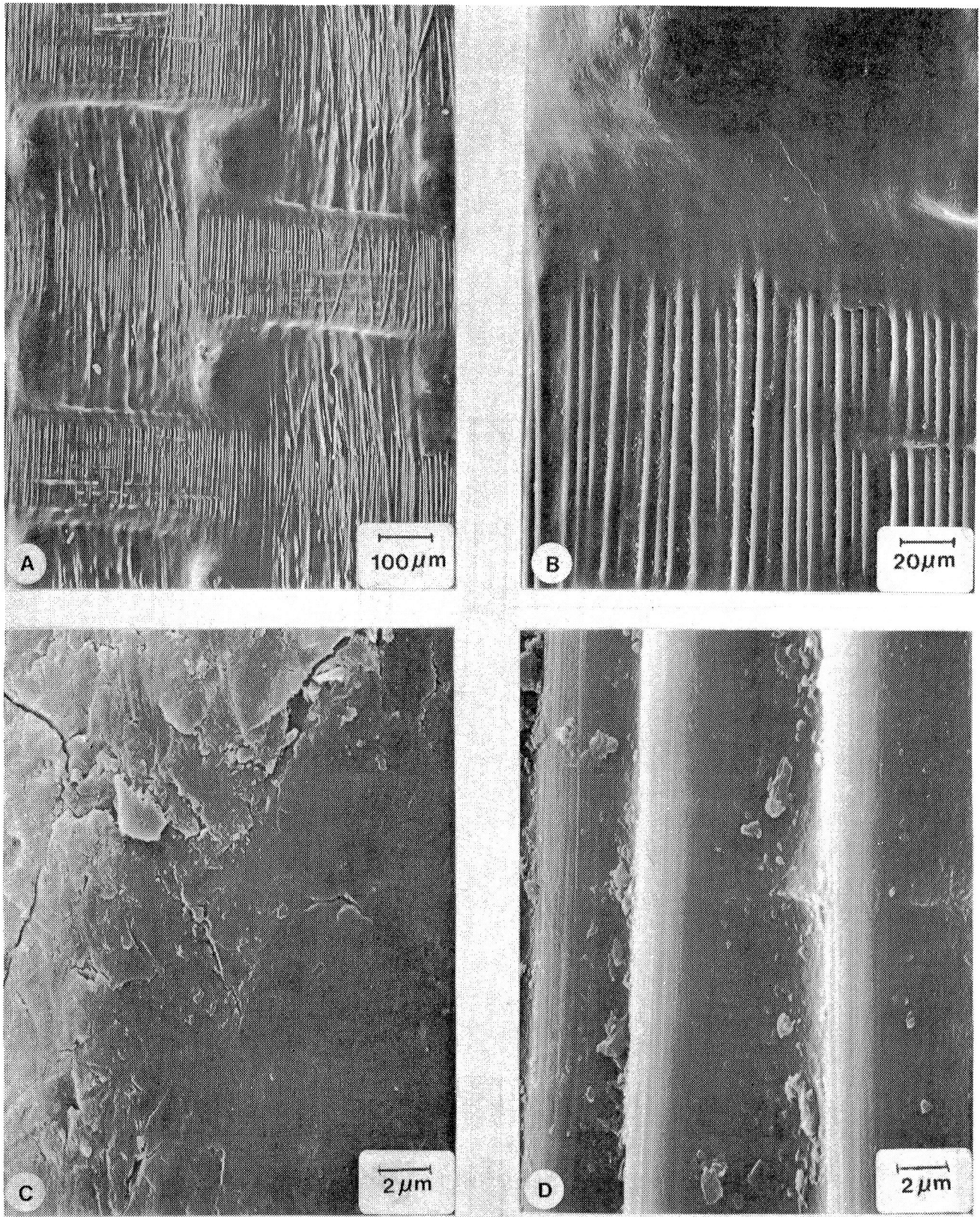


FIGURE 4. SEM PHOTOMICROGRAPHS OF AS-RECEIVED SAMPLE #1A.

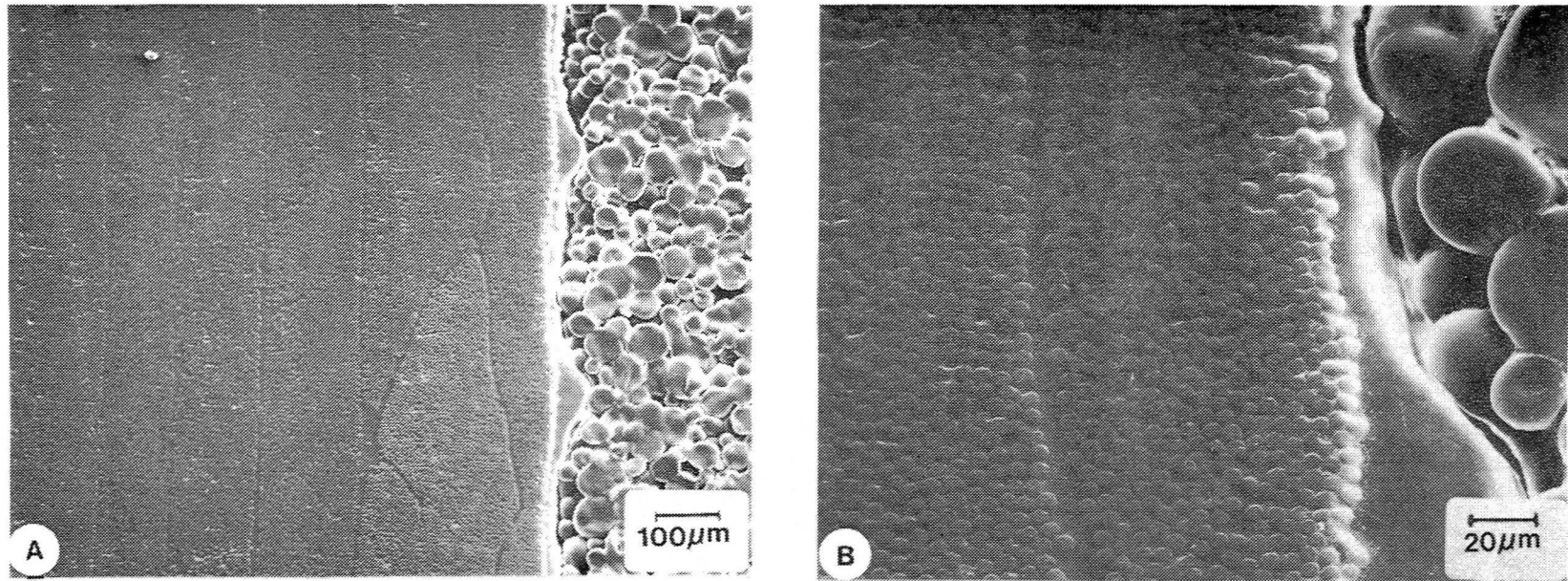


FIGURE 5. SEM PHOTOMICROGRAPHS OF EDGE VIEW OF AS-RECEIVED SAMPLE #1A.



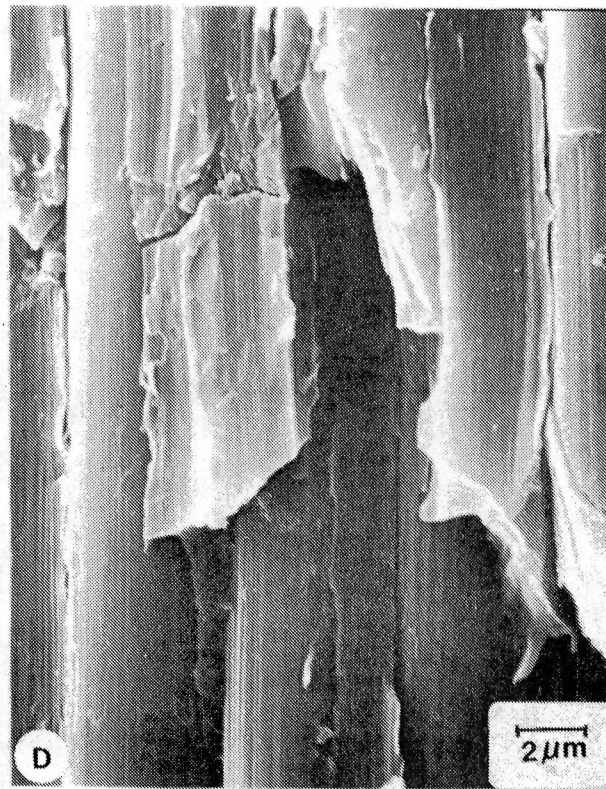
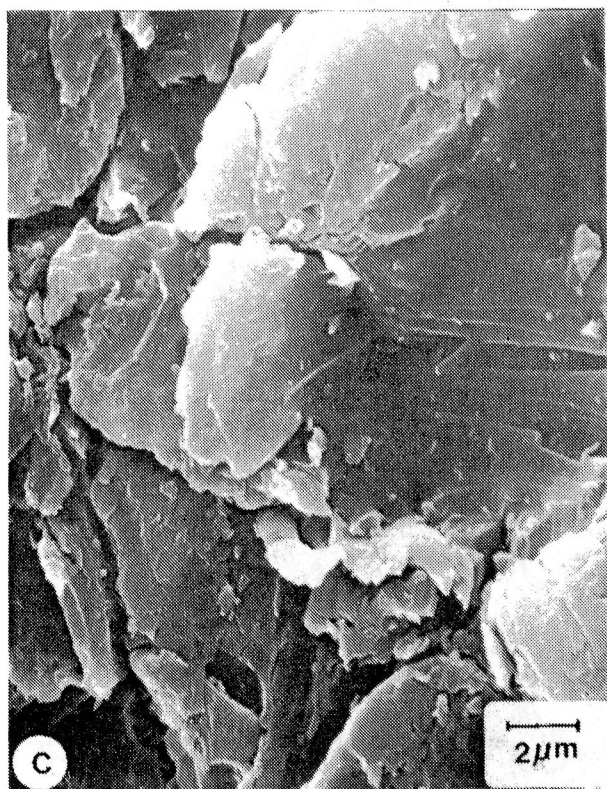
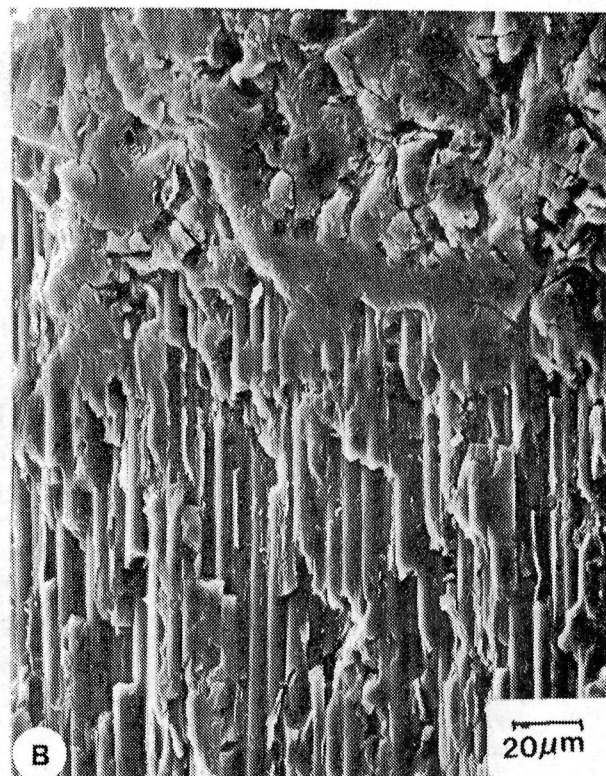
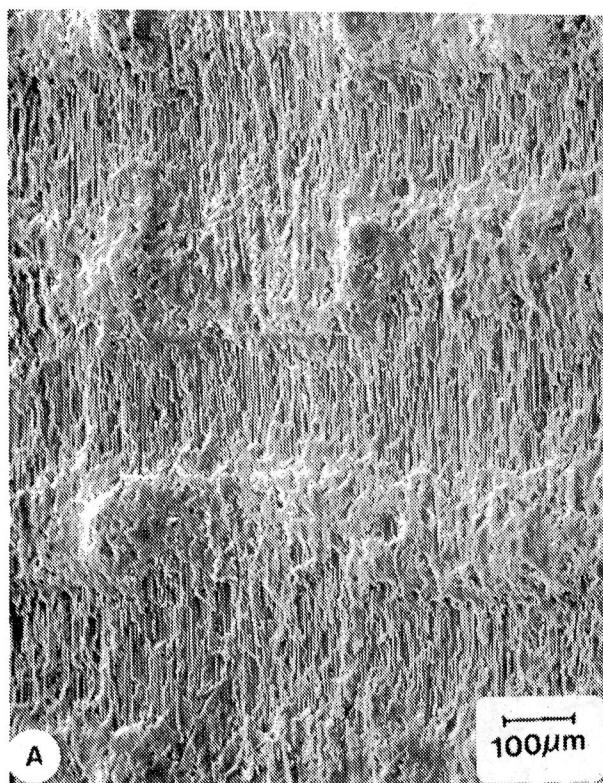


FIGURE 6. SEM PHOTOMICROGRAPHS OF 120  $Al_2O_3$  GRIT BLASTED SAMPLE #2.

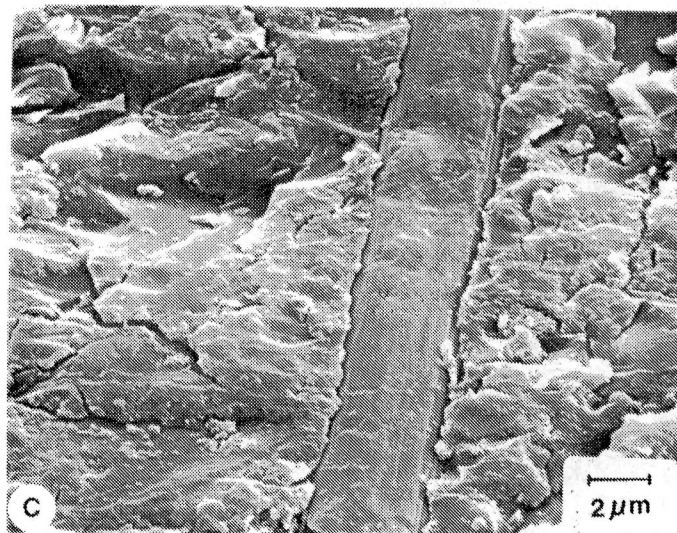
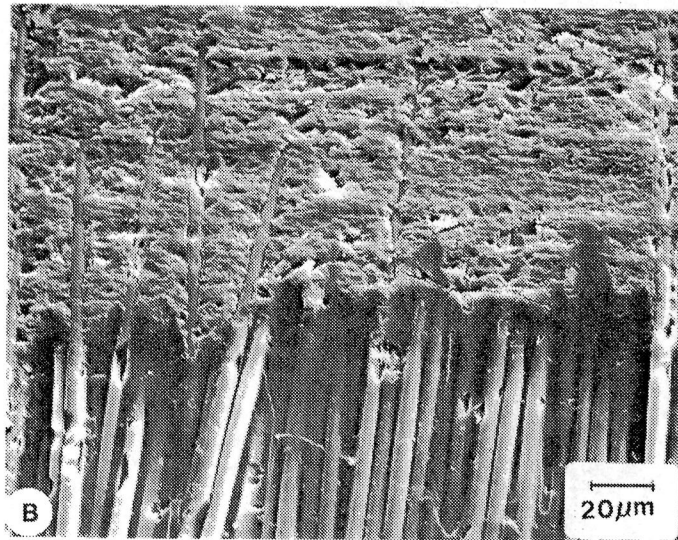
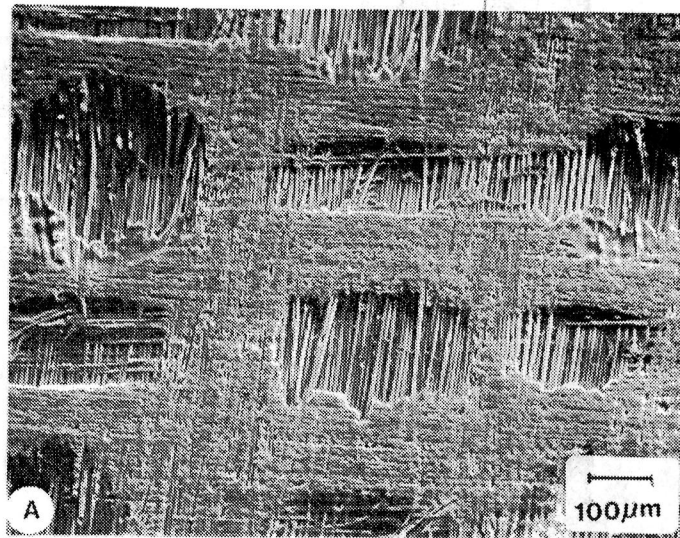


FIGURE 7. SEM PHOTOMICROGRAPHS OF 600 SIC HANDSANDED SAMPLE #5.

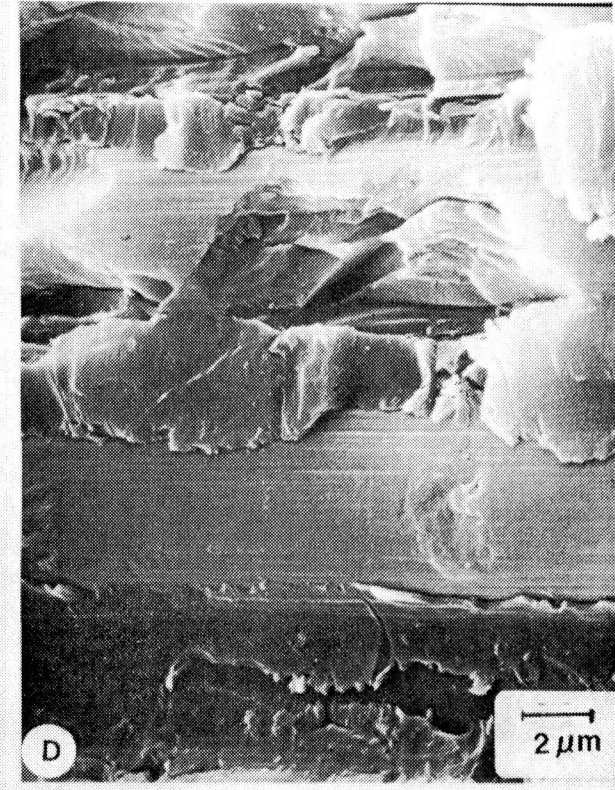
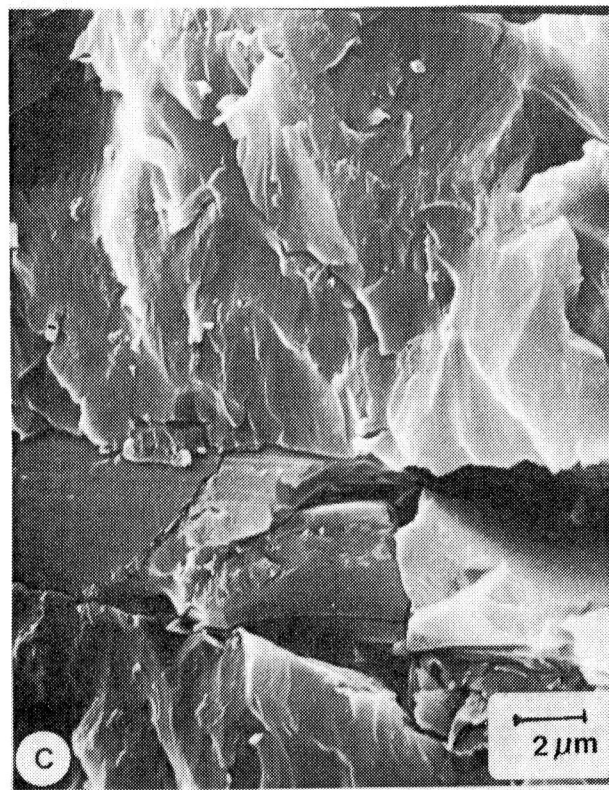
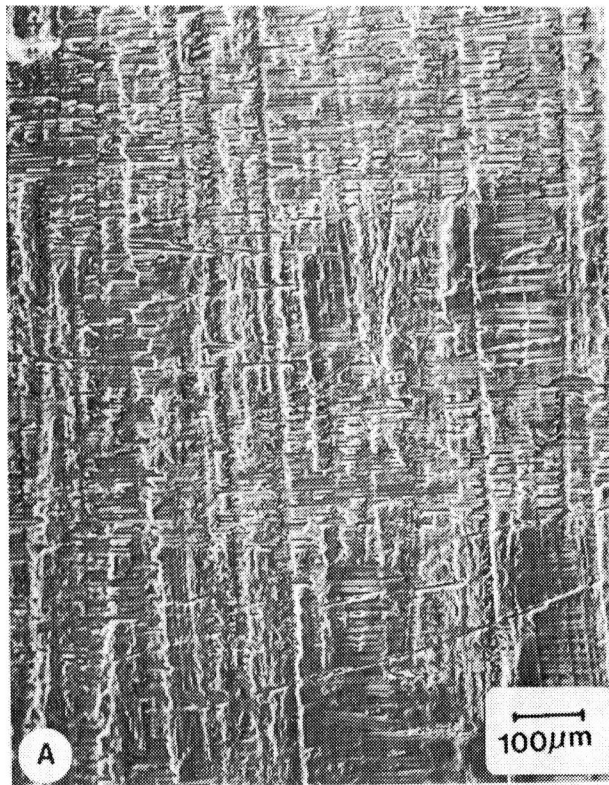


FIGURE 8. SEM PHOTOMICROGRAPHS OF 180 SiC HANDSANDED SAMPLE #6.

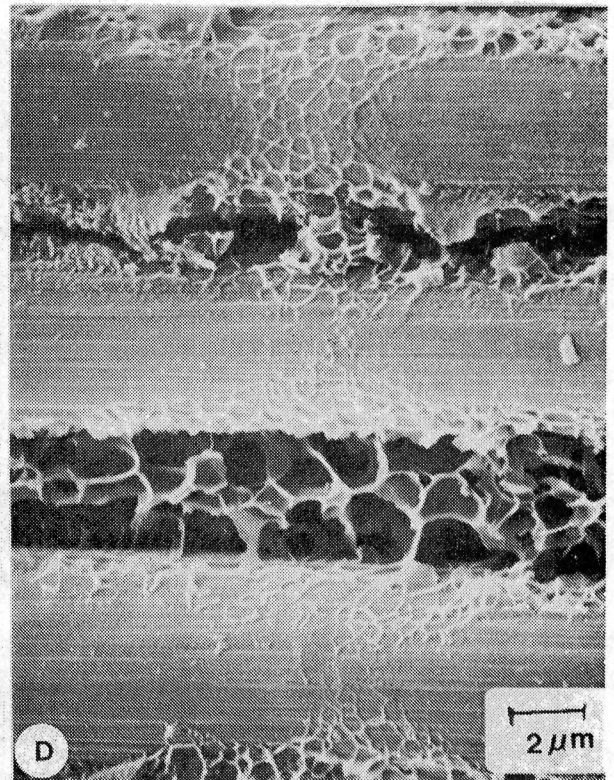
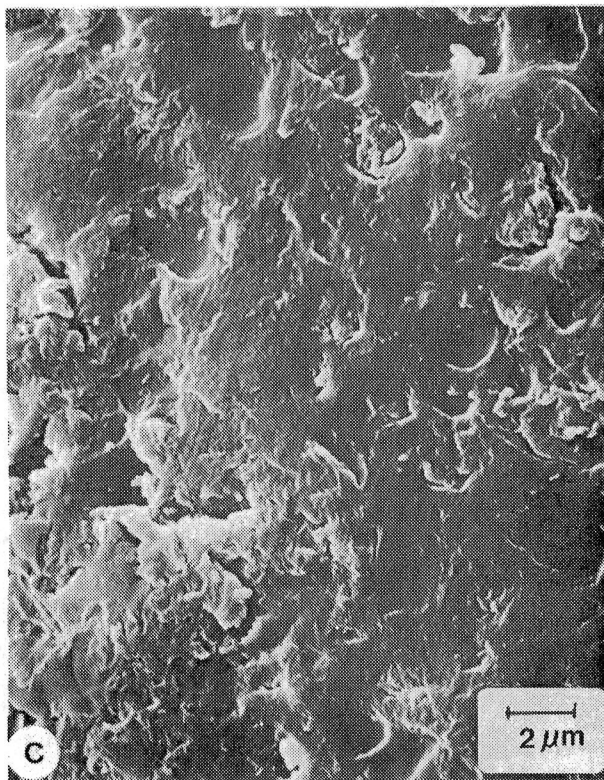
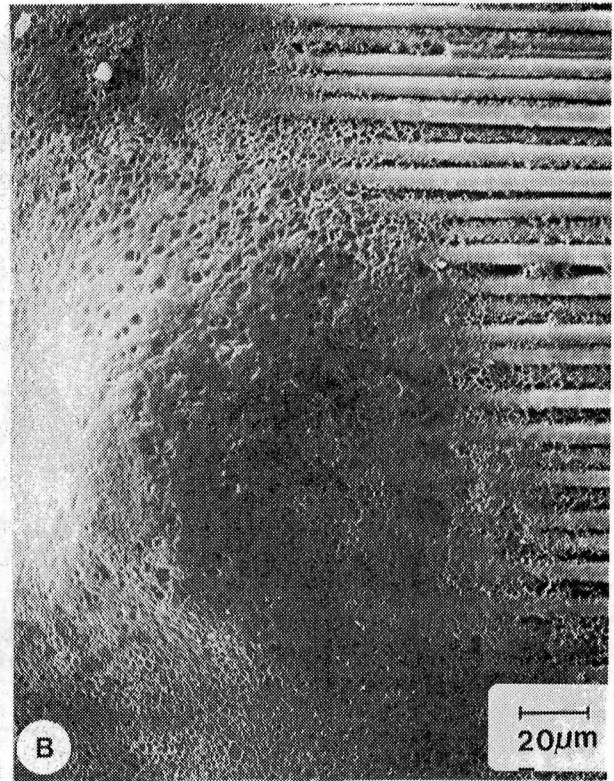


FIGURE 9. SEM PHOTOMICROGRAPHS OF FLASHBLAST #3 SAMPLE #12W.

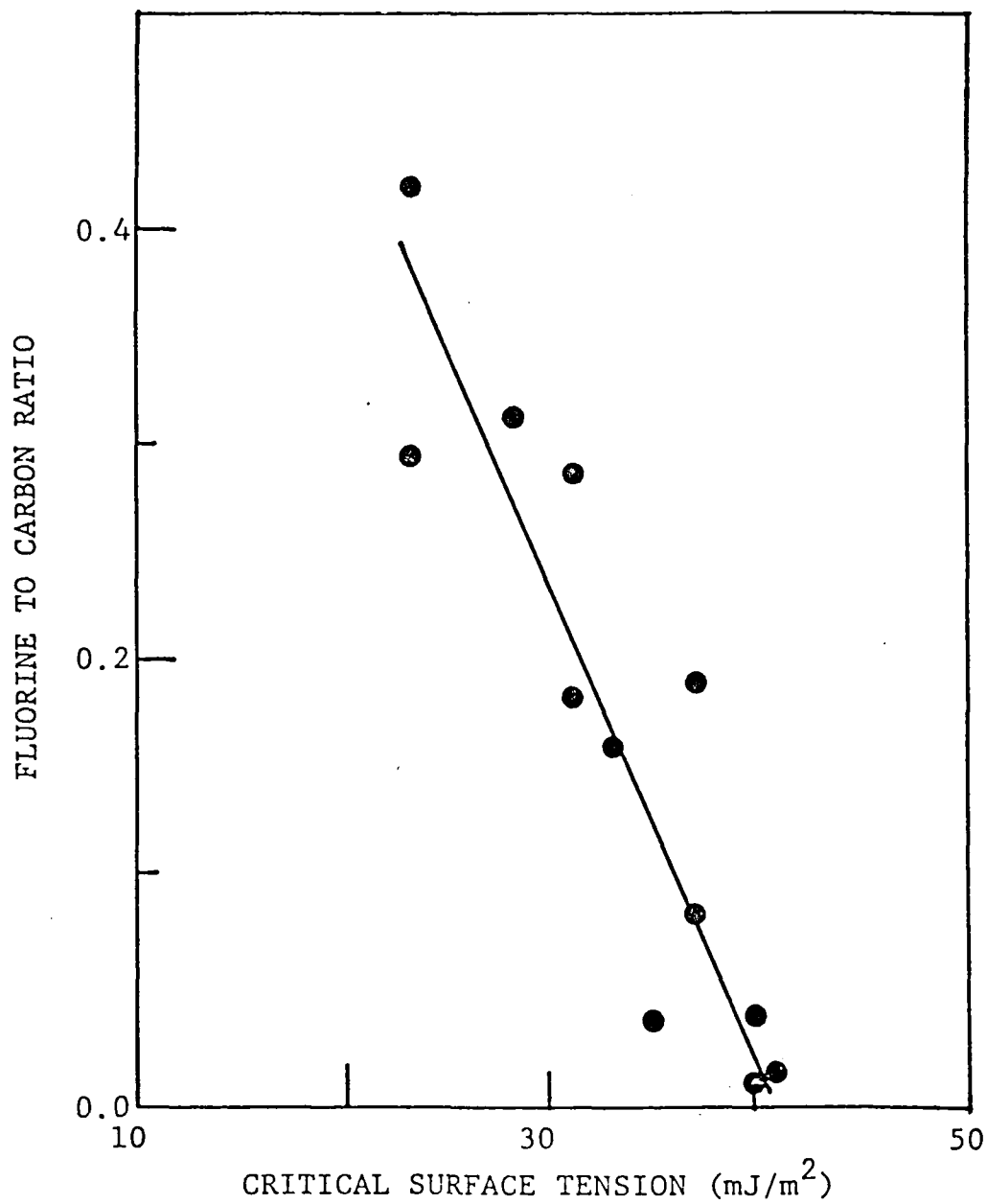


FIGURE 10. XPS FLUORINE TO CARBON RATIO AS A FUNCTION OF THE CRITICAL SURFACE TENSION OF PRETREATED COMPOSITES.

1. Report No. NASA TM-85700		2. Government Accession No.		3. Recipient's Catalog No.	
4. Title and Subtitle Surface Analysis of Graphite Fiber Reinforced Polyimide Composites				5. Report Date October 1983	
				6. Performing Organization Code 506-53-23-06	
7. Author(s) D. L. Messick,* D. J. Progar,** and J. P. Wightman*				8. Performing Organization Report No.	
				10. Work Unit No.	
9. Performing Organization Name and Address NASA Langley Research Center Hampton, VA 23665				11. Contract or Grant No.	
				13. Type of Report and Period Covered Technical Memorandum	
12. Sponsoring Agency Name and Address National Aeronautics and Space Administration Washington, DC 20546				14. Sponsoring Agency Code	
15. Supplementary Notes *VPI&SU Blacksburg, VA 24061      **NASA-Langley Research Center Hampton, VA 23665 Use of commercial products or names of manufacturers in this report does not constitute official endorsement of such products or manufacturers, either expressed or implied, by the National Aeronautics and Space Administration. Presented at the 15th National SAMPE Technical Conference on October 4-6, 1983 in Cincinnati, OH.					
16. Abstract Several techniques have been used to establish the effect of different surface pre-treatments on graphite-polyimide composites. Composites were prepared from Celion 6000 graphite fibers and the polyimide LARC-160. Pretreatments included mechanical abrasion, chemical etching and light irradiation. Scanning electron microscopy (SEM) and X-ray photoelectron spectroscopy (XPS) were used in the analysis. Contact angles of five different liquids of varying surface tensions were measured on the composites. SEM results showed polymer-rich "peaks" and polymer-poor "valleys" conforming to the pattern of the release cloth used during fabrication. Mechanically treated and light irradiated samples showed varying degrees of polymer peak removal, with some degradation down to the graphite fibers. Minimal changes in surface topography were observed on chemical pretreatment. XPS spectra showed that half of the samples contained high concentrations of surface fluorine even after pretreatment. The light irradiation pretreatment was most effective at reducing surface fluorine concentrations whereas chemical pretreatment was the least effective. Critical surface tensions correlated directly with the surface fluorine to carbon ratios as calculated from XPS.					
17. Key Words (Suggested by Author(s)) graphite-polyimide composites, surface analysis, SEM, XPS, and critical surface tension.			18. Distribution Statement Unclassified-unlimited Subject Category 24		
19. Security Classif. (of this report) Unclassified		20. Security Classif. (of this page) Unclassified		21. No. of Pages 20	22. Price A02

)

